ELSEVIER

Journal of Nuclear Materials 307–311 (2002) 852–861

journal of nuclear materials

www.elsevier.com/locate/jnucmat

Atomistic study of the generation, interaction, accumulation and annihilation of cascade-induced defect clusters

Yu.N. Osetsky [a,*], D.J. Bacon [a], B.N. Singh [b], B. Wirth [c]

[a] *Department of Engineering, Materials Science and Engineering, The University of Liverpool, Brownlow Hill, Liverpool L69 3GH, UK*
[b] *Department of Materials Research, Risø National Laboratory, P.O. Box 49, DK-4000 Roskilde, Denmark*
[c] *Lawrence Livermore National Laboratory, Livermore, CA 94551, USA*

Abstract

Recent theoretical calculations and atomistic computer simulations have shown that glissile clusters of self-interstitial atoms (SIAs) play an important role in the evolution of microstructure in metals and alloys under cascade damage conditions. Over the past decade or so, the properties of SIA clusters in fcc, bcc and hcp lattices have been widely studied. In this paper we review key properties of these defects and also those of vacancy clusters formed directly in cascades, and present an atomic-level picture based on computer modelling of how these properties may change in the presence of other defects, impurities, stress fields, etc. We then examine the role of cluster properties and the consequences of their interactions in the process of damage accumulation and changes in mechanical and physical properties. We focus on the formation of defect clusters (e.g. dislocation loops and stacking fault tetrahedra (SFT)) and their segregation in the form of rafts of dislocation loops and atmospheres of loops decorating dislocations. Finally, we address the problem of radiation hardening by considering interactions between mobile dislocations and defect clusters (e.g. SIA dislocation loops, SFT and microvoids) produced during irradiation.

1. Introduction

Recent studies of radiation effects in metals have highlighted the important role of primary defect clusters – 'primary' in the sense that they are produced directly in displacement cascades – in microstructural evolution and changes in properties of materials subjected to irradiation with energetic particles. Atomic-level modelling by computers using the molecular dynamics (MD) technique has demonstrated that a significant fraction of defects formed in the high-energy displacement cascades is in the form of clusters [1,2]. The properties of clusters of vacancies and self-interstitial atoms (SIAs) have extremely important effects on further evolution of defect microstructure for they are highly stable [3,4] and exhibit fast motion by thermally activated one-dimensional (1-D) glide [4–9].

The fact that small glissile SIA clusters are produced directly in displacement cascades has significant impact on damage accumulation behaviour, and thus physical and mechanical properties, of materials under cascade damage conditions. In recent years it has been demonstrated, for example, that the stability and 1-D transport of SIA clusters provide the main driving force for the evolution of void swelling and that both of these properties can be taken into account quantitatively in the theoretical treatments based on the production bias model (PBM) [10]. It has also been shown that the 1-D transport of SIA clusters lead to segregation of SIA clusters and dislocation loops in the form of dislocation decorations and rafts of loops [11–13]. Furthermore, the segregation of the SIA loops forms the basis of the cascade-induced source hardening (CISH) model of

* Corresponding author. Tel.: +44-151 794 4662; fax: +44-151 794 4675.
E-mail address: osetsky@liverpool.ac.uk (Yu.N. Osetsky).

0022-3115/02/$ - see front matter
PII: S0022-3115(02)01094-2

radiation hardening and yield drop, associated with the initiation of plastic flow localisation in the form of 'cleared channels' at temperatures below the recovery stage V [14]. In all these cases loop–loop and loop–dislocation interactions play a vital role. In the earlier work on the PBM and CISH models, the strength of these interactions were calculated using the isotropic linear elasticity theory, which may not necessarily be accurate for the interactions at close distances (of the order of loop size) between loops or loops and an edge dislocation and, therefore, should be tested, e.g. by comparing with MD calculations [15,16].

The generally accepted philosophy for study of evolution of microstructure and its effect on change of properties is to use a multiscale approach, when the physical phenomena are characterised by specific time and space scales and are investigated by relevant techniques. The place of atomic-level modelling includes studies of primary defect production, defect properties, reactions between defects and mechanisms of interactions affecting the mechanical properties, e.g. interactions with the core of moving dislocations. In this paper we present an overview of recent results in these areas. A variety of different models are required to study the different atomic-level phenomena, and a short description of them is presented in the following section.

2. Atomistic models

2.1. Defect production

Typical MD simulation of displacement cascades involves crystallites containing up to few million atoms, with periodic boundary conditions and, sometimes, with the application of electron–phonon coupling [17] or/and with a thermal bath on the crystal periphery [18,19]. By now, cascades of primary-knock-on-atom (PKA) energy, E_{PKA}, up to 50 keV have been simulated in different bcc, fcc and hcp metals over a wide temperature range [1,2,17–30]. The cascade region is usually simulated till its temperature drops down to the ambient, though in some cases short-term post-cascade annealing has been modelled to investigate the behaviour of clusters over few hundreds picoseconds [23]. The standard output of cascade simulations includes the total number of the surviving vacancy and interstitial defects at the end of cascade cooling phase ($2N_{\mathrm{F}}$), the fraction of vacancies and SIAs formed in clusters ($\varepsilon_{\mathrm{v}}, \varepsilon_{\mathrm{i}}$), information on the size distribution and the structure of these clusters (sessile, glissile, Burgers vector) and atomic squared displacements (for characterisation of mixing). Few tens of events at each condition (PKA energy and direction, temperature) must be simulated to achieve statistically representative results [2,23].

2.2. Cluster properties

Modelling of defect cluster properties includes two different approaches. Static modelling – in which the atoms have no kinetic energy and equilibrium is computed by minimisation of the crystal potential energy – is used to study the energy and structure of clusters, their interaction energy with other defects and stress and displacement fields. SIA and vacancy clusters and dislocation loops containing up to several hundred point defects have been modelled in crystallites containing up to a few million atoms using periodic or fixed boundaries [3,4]. Dynamic modelling by MD – in which the crystal has non-zero temperature – is used to study transport properties and mechanisms of cluster motion in periodic crystallites. These simulations require smaller crystallites (up to a hundred thousand atoms), but the nature of the phenomena is such that the simulated time is usually much longer than for cascades, lasting up to several tens of nanoseconds. Motion of clusters of up to a few hundred SIAs and vacancies [5–9], and statics and dynamics of cluster–cluster interactions [15,16,31] were studied in bcc, fcc and hcp metals.

2.3. Dislocation-cluster interactions

This is a relatively new area of atomistic modelling and involves both static and dynamic approaches. It employs periodicity along the straight dislocation line and needs the boundaries in the other two directions either fixed, with atoms displaced according to elasticity theory [15,16,32], or flexible, with atoms able to respond to unbalanced forces using either lattice or elastic Green functions [33,34]. The static modelling has been used to study interactions between edge dislocations and defect clusters (voids, stacking fault tetrahedra (SFT), SIA clusters) in bcc and fcc metals. The advantage of static models is that their results can be compared with continuum elasticity theory (stress–strain behaviour, energy and plastic deformation during the dislocation–obstacle interaction [35]), and they can also be used to describe interactions necessary for higher level methods, e.g. continuum dislocation dynamics modelling. The newest application of MD is related to dynamics of dislocation–obstacle interactions at non-zero temperature using modifications of an earlier model [36] for an edge dislocation where periodicity along the direction of the Burgers vector was used. The method actually simulates a periodic array of dislocations and the accuracy for a single dislocation depends on the distance between dislocations, e.g. the size of simulated crystal. Current progress in computer power allows modelling of systems of realistic size, e.g. spacing between dislocations and between obstacles about l00 nm, to be carried out in crystals of about ten million atoms over several hundred picoseconds [31,35,36]. Projected improvement in

computer technology should offer the possibility of using relatively simple and fast computer models for dislocations when periodicity along the glide direction permits long-range motion. So far, such studies have been limited to dynamics of edge dislocations in bcc and fcc metals.

2.4. Potentials of interatomic interactions

The validity of the interatomic potential (IAP) is an important issue in any atomic-scale model, for the IAP determines all the properties of the simulated system. We refer to reviews of the subject [36–38], and only mention that the most commonly used lAPs are based on the long-ranged pair potentials [39] created within the generalized pseudopotential model by Moriarty [40] and many-body approximation of embedded atom model [38], Finnis–Sinclair-type potentials [41]. Other types, such as tight-binding models, bond order potentials, general many-body potentials, are not being used extensively in the large-scale atomic modelling, for this requires too high computational resources.

3. Defect production in displacement cascades

Vast experience and much data have been obtained during the last decade on the nature of primary damage in high-energy displacement cascades in the bulk of pure bcc [1,19,20], fcc [1,2,17,18,21–23] and hcp [24–26] metals, some binary (Fe–Cu [27]) and ordered (Ni_3Al [28,29]) alloys, and near metal surfaces [25,26,30]. The basic processes have been clarified and the results are in overall agreement with experimental observations. More detailed comparison between modelling and experimental data is presented in [2]: here we present the main conclusions.

3.1. Defect production

One of the most significant findings of atomistic modelling is that an extensive amount of recombination of SIAs and vacancies occurs during the cooling down stage of high-energy cascades. As a consequence, in all metals and alloys modelled so far, the total number, N_F, of point defects (vacancy or SIA) surviving at the end of the cascade process is significantly lower than the number of atomic displacements, N_{NRT}, predicted by the NRT model [44]. The defect production efficiency, N_F/N_{NRT}, depends strongly on PKA energy, less on material and weakly on ambient temperature [1].

3.2. Intracascade clustering

The occurrence of intracascade clustering is another important finding of atomistic modelling. The collapse of cascades into vacancy clusters was demonstrated in some metals on the basis of low temperature experiments [45] and used in theoretical treatment of void swelling [46]. The direct formation of clusters of SIAs in cascades was predicted by both MD modelling of displacement cascades [21] and diffusion-based theoretical calculations [47] in the early 1990s and then was confirmed by TEM [48]. Since then the intracascade clustering of vacancies and SIAs has been substantiated in a variety of metals using MD simulations.

It can be concluded that SIA clusters are formed in displacement cascades in all bcc, fcc and hcp metals with a high efficiency. For example, in Cu, each cascade of 10–20 keV PKA energy yielded one to two SIA clusters of mean size of ~5–6 defects (on average) [2]. The fraction of SIAs in clusters, ε_i, was found to be in the range of 50–60%. The majority of SIA clusters have the form of glissile perfect dislocation loops. Clusters in sessile configuration have also been observed in MD simulations, to an extent which is metal-dependent. The fraction is the lowest, only a few per cent, in bcc metals and consists of metastable three-dimensional (3-D) clusters [49], and the highest, up to ~30–40%, in low stacking fault energy fcc metals and includes stable faulted Frank dislocation loops [2,23]. The sessile fraction in hcp metals lies between these extremes.

Production of vacancy clusters is strongly dependent on the crystal structure. For example, large compact clusters are observed only in simulations of fcc and hcp metals. In fcc Cu they are perfect or truncated SFTs [33,50,51] while in hcp Zr they are planar defects similar to prism or basal dislocation loops [24,25]. No large compact planar or 3-D vacancy clusters have been observed in bcc metals. Instead, very loose complexes of vacancies in second and higher order neighbour shells have been reported [20,52,53]. The best statistics of cascade defects was obtained for Cu [2] where, on average, each cascade of 10–20 keV PKA energy produces one cluster of about 5 vacancies, and in total about 25% of surviving vacancies was found to be contained in the clusters.

3.3. Temperature effects

No significant effect of temperature on the total number of defects produced in cascades has been reported, but there is a statistically significant effect on defect clustering [1,2,19,26,28]. For example, in Cu the number of vacancy and interstitial clusters per cascade decreases at high temperature while the number of defects per cluster increases [2]. The difference between vacancy and interstitial clustering was found to be in the temperature dependence of the defect fraction contained in clusters: ε_i increases with temperature while ε_v is rather insensitive.

4. Properties of defect clusters

Recognition that intracascade clustering of both SIAs and vacancies is substantial has initiated extensive investigations of the atomic-level properties of such clusters. These studies were mainly focused on structure and stability of vacancy and interstitial clusters [3,4,51–58] and transport properties of SIA clusters [4–9].

4.1. Vacancy clusters

Stability of vacancy clusters is strongly dependent on crystal structure. The most stable vacancy clusters in fcc Cu are in the form of SFTs [3,56], which in MD modelling are stable up to 1000 K for at least a few ns. Faulted Frank vacancy dislocation loops in Cu are also very stable and tend to dissociate into SFTs. An example of stability of vacancy clusters in Cu from [56] is presented in Fig. 1. Studies of hcp Zr [57,58] show that planar vacancy clusters in the form of perfect dislocation loops in prism planes and faulted loops in basal plane are stable. The situation in bcc metals, particularly in Fe, is more complex. Small clusters (<30 vacancies) are metastable in the form of planar or 3-D, void-like configurations, and during high temperature annealing transform into cloud-like complexes. Such loose clusters are mobile in the bcc lattice [3,59,60]. Larger clusters can be stable compact 3-D voids or perfect $1/2\langle 1\,1\,1\rangle$ and $\langle 1\,0\,0\rangle$ edge dislocation loops [7,53].

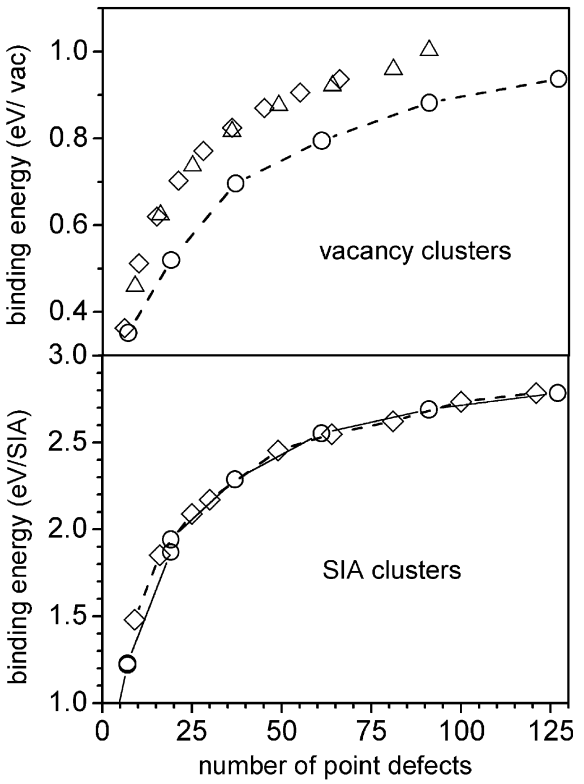

Fig. 1. Binding energy of SIA and vacancy clusters in Cu [4,56]. Circles – faulted $1/3\langle 1\,1\,1\rangle$ Frank loops, diamonds – rhombus-shaped $\_\langle 1\,1\,1\rangle$ perfect loops, triangles – SFTs.

Attempts have been made to study nucleation of vacancy clusters in different metals under conditions of very high vacancy supersaturation. It was demonstrated that vacancy-rich regions in metals collapse into the highly stable configurations of SFTs and faulted Frank loops in Cu [3,50,51], basal and prism loops in Zr [57] and perfect loops in $\{1\,1\,1\}$ and $\{1\,0\,0\}$ planes in Fe [52,53], depending on the level of supersaturation. There was no evidence for the formation of compact 3-D void-like configurations in any of the crystal structures, which may be related to the limited time-scale of atomistic studies, of the order of nanoseconds, or the impossibility of void nucleation without the help of gaseous impurities.

A recent significant achievement related to vacancy clusters provides an explanation of the growth mechanism of SFTs in Cu [56]. It was found that growth of an SFT occurs by stair-rod dislocation jog propagation over the SFTs facetted surface. The growth of large SFTs is suppressed due to difficulties in propagation of long jogs, and this makes the size distribution limited to a few nanometres. This mechanism explains experimental observation that SFT size distribution is independent of the irradiation conditions [61].

4.2. Interstitial clusters

Interstitial clusters in bcc, fcc and hcp structures have been extensively studied over the last decade. The structure and energy of $1/2\langle 1\,1\,0\rangle$ perfect and $1/3\langle 1\,1\,1\rangle$ faulted dislocation loops in Cu, $1/2\langle 1\,1\,1\rangle$ and $\langle 1\,0\,0\rangle$ perfect loops in Fe and $1/2\langle 1\,1\,\bar{2}\,0\rangle$ perfect loops in Zr have been investigated [4–8,36,62,71]. The thermally activated 1-D glide of all these perfect dislocation loops containing up to a few hundred SIAs, i.e. up to a few nanometres in diameter, was observed [5–9,62–65]. The following conclusions can be drawn.

(a) All types of SIA clusters in all metal structures have very high binding energy, of the order 2–3 eV/SIA (Fig. 1). They cannot dissociate thermally, but can transform from metastable into stable configurations.
(b) The most stable clusters are nuclei of perfect dislocation loops, i.e. Burgers vector $1/2\langle 1\,1\,0\rangle$ in fcc (Cu), $1/2\langle 1\,1\,1\rangle$ and $\langle 1\,0\,0\rangle$ in bcc (Fe) and $1/2\langle 1\,1\,\bar{2}\,0\rangle$ in hcp (Zr). These clusters can be described as compact planar sets of crowdions with their axis along the Burgers vector direction [4,9,58] and are intrinsically glissile.
(c) Sessile, stable loops are formed in fcc ($1/3\langle 1\,1\,1\rangle$ faulted Frank loops) and hcp ($1/2\langle 0\,0\,0\,1\rangle$ faulted

basal loops) metals but do not form in bcc crystals where all stable clusters are intrinsically glissile. Large rhombus-shaped clusters (with sides along $\langle 1\,1\,2\rangle$) in Cu can dissociate along their glide prism. Such clusters become sessile due to the formation of stair rod dislocations at their corners [4,7,8].

(d) Small perfect dislocation loops perform fast thermally activated 1-D motion. Mobility decreases with increasing size, but the activation energy does not depend on size and is close to that of the individual crowdion of the corresponding type, e.g. ~0.02–0.05 eV [6–9]. The thermally activated motion of clusters is suppressed at large size, e.g. above ~300 SIAs for $1/2\langle 1\,1\,1\rangle$ clusters in Fe and ~120 SIAs for $1/2\langle 1\,1\,0\rangle$ clusters in Cu [64].

(e) The thermally activated motion of clusters is unlikely to be described by conventional diffusion because the activation energy is lower than the thermal energy of atoms at ambient temperature. Nevertheless, attempts have been made to parameterise such motion as correlated 1-D diffusion, and the jump frequency of the centre of the mass of clusters, correlation factor and effective migration energy have been estimated for clusters containing up to 91 SIAs in Fe, Cu and Zr [6–9,64]. Qualitatively similar results were obtained in all cases and the example for Fe is presented in Fig. 2. It has been shown that the mechanism of cluster motion can be described as nearly stochastic jumps of crowdions with the probability to move the cluster centre of mass being inversely proportional to the number of SIAs in the cluster [65]. The effective correlation factor is significantly larger than unity, implying preferential motion of the cluster in one direction over large distance, e.g. up to tens of nanometers for tens of picoseconds. The physical basis for the fast thermally activated glide of SIA clusters is not yet clarified, but the parameters obtained [6–9,64] can be used in theoretical and phenomenological models of microstructure evolution and damage accumulation [66].

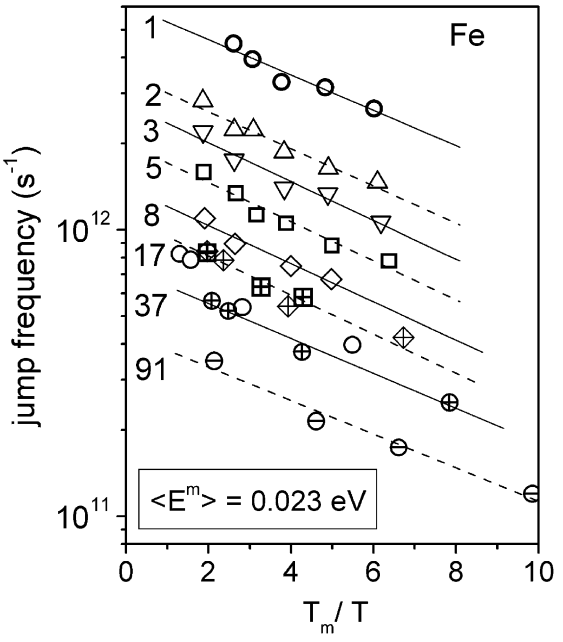

Fig. 2. Jump frequency of SIA clusters in Fe. The number of SIAs is indicated on the left of each Arrhenius-like dependence [8].

5. Interactions between defect clusters

It is clear from the preceding description that the importance of glissile SIA clusters arises from their high stability, fast mobility and specific long-range interactions along their glide path due to their 1-D motion. Hence, interactions of such clusters between themselves, with sessile clusters and dislocations are of importance for any model attempting to predict the microstructural evolution during irradiation under cascade damage conditions. A great variety of interactions between SIA clusters and other microstructural components have been studied already by atomic modelling and can be separated into two groups.

5.1. Reactions

To this group we attribute interaction between clusters and point defects, which may lead to growth and shrinkage; interaction between clusters, which may result in coalescence or annihilation, and interactions that can induce changes in clusters properties (e.g. sessile $\Longleftrightarrow$ glissile transformations).

Interactions of this type are widely observed in cascade simulations where the probability of such events is increased by the high local concentration of defects. For example, growth, shrinkage and coalescence of glissile perfect $1/2\langle 1\,1\,1\rangle$ SIA clusters due to interactions with point defects (vacancies and SIAs) and other clusters, and the formation of sessile 3-D clusters were observed in simulations of high energy cascades in Fe [49] and Cu [2,23,67], where they may form several local stacking-faults in different $\{1\,1\,1\}$ planes. Due to existence of stable sessile configuration of SIA clusters in Cu, e.g. Frank loops, the probability of observing sessile SIA clusters in this metal is much higher than in Fe. An example where a group of small glissile SIA clusters form a Frank-type defect in a 20 keV cascade in Cu is presented in Fig. 3 [2].

MD study of interactions between glissile clusters with intersecting glide prisms in Fe and Cu has shown that the final result depends on cluster size, temperature and cluster orientation [31]. In general, for small clusters

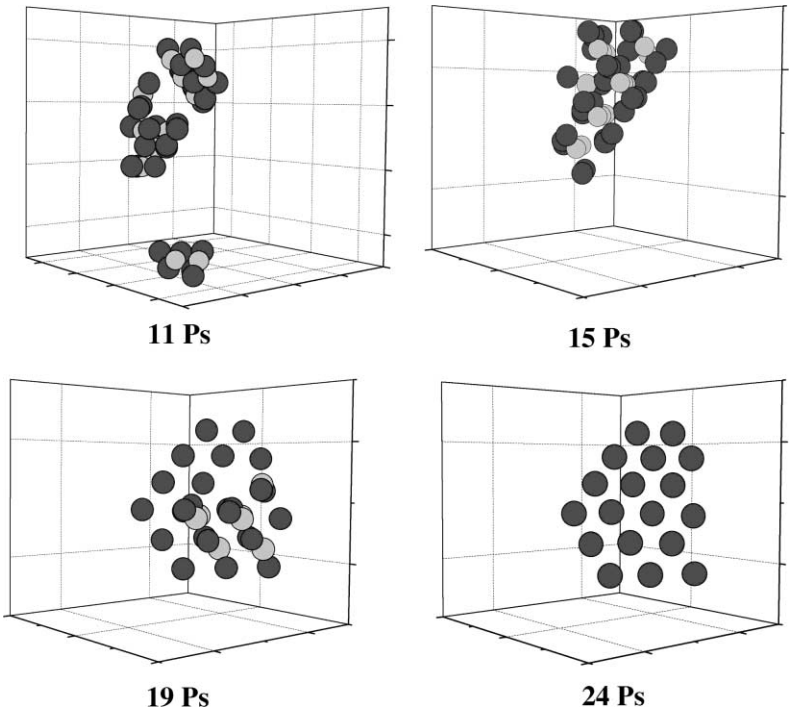

Fig. 3. Three $1/2\langle 1\,1\,0\rangle$ glissile SIA clusters coalesced to form the nucleus of a sessile $1/3\langle 1\,1\,1\rangle$ Frank loop during simulation of a 20 keV cascade in Cu [2]. The time after the PKA impact is indicated for each configuration. Dark spheres are interstitial atoms, light spheres are vacant sites.

and high temperature, the probability that one of them (usually the smaller) changes its Burgers vector to coalesce with the other increases. Large clusters may combine to form immobile complexes and the probability for this is higher in Cu than in Fe.

Important interactions may occur when the mobility of glissile SIA clusters is reduced or when they become immobile without change of structure. Such effects were observed for $1/2\langle 1\,1\,1\rangle$ SIA cluster in Fe interacting with a vacancy [68] and an impurity atom [69]. In particular, a significant decrease in the cluster mobility occurs when an impurity atom interacts with the cluster and becomes trapped at its edge. This effect has been observed in the simulation of a carbon solute atom and a $1/2\langle 1\,1\,1\rangle$ glissile cluster in Fe [69]. Whilst the cluster became essentially immobile (at 300 K), the carbon atom maintained its mobility around the cluster edge by core diffusion. The mobility of a cluster–solute complex is controlled by the solute, which, at high enough temperature, could be dragged by the cluster one-dimensionally towards the latter's own sink.

5.2. Creation of specific microstructures

Interaction between glissile clusters/loops with parallel Burgers vectors, **b**, leads to formation of extended complexes. Some cases were studied by statics and MD in [16,31]. It was found that $1/2\langle 1\,1\,1\rangle$ SIA clusters in Fe, with no overlapping glide prisms, attract each other and form a stable complex. The nature of the clusters does not change, i.e. they are still glissile, but the mobility of the complex depends on the number and size of the clusters: the complex retains mobility if the number of clusters is small (<5) and the total number of SIAs is <300, but becomes immobile for larger numbers. A complex can grow further, attracting more glissile clusters with the same **b**, thereby creating a raft of clusters/dislocation loops. The interaction energy obtained in the atomistic modelling was compared with that estimated from elasticity theory for infinitesimal and finite size dislocation loops, and whereas the long-range interaction can be well approximated within the elasticity theory, the short-range interaction was found to be stronger in the atomistic model [16]. This type of interaction depends on the crystal lattice structure, for in fcc Cu $1/2\langle 1\,1\,0\rangle$ glissile SIA clusters repel each other at large distances but attract at short distances, creating an immobile complex even for two small clusters [31]. The reasons for such behaviour are not yet understood and cannot be clarified within the isotropic elasticity theory. Nevertheless, the effects found in modelling are qualitatively consistent with experiments in which rafts of dislocation loops are observed in bcc [12–14,70] but not in fcc metals.

Another pertinent interaction is that between a glissile SIA cluster and an edge dislocation when both have the same **b**. This interaction was studied by atomistic modelling and isotropic elasticity in [15,16] for $\mathbf{b} = 1/2\langle 1\,1\,1\rangle$ in Fe and $\mathbf{b} = 1/2\langle 1\,1\,0\rangle$ in Cu. In Fe the short-range interactions are stronger in the atomic model while the long-range interactions can be described with reasonably by elasticity theory, even within the infinitesimal dislocation loop approximation. The situation is more complicated in Cu due to the enhanced dissociation of perfect clusters/loops in the stress field of a dislocation (see Fig. 4). As a result the interaction energy, E_{INT}, is significantly higher at short distances where such dissociation may occur in clusters of sizes too small to dissociate in isolation (e.g. [4]). In general, these results confirm that short-range interactions are too complicated to consider in elasticity theory. However, for long-range interactions, when cluster-dislocation separation is much larger than the cluster size and the defects have little effect on each others properties, elasticity calculations give good results when dislocation parameters such as core energy and radius are estimated from atomic-level modelling. This interaction is very long-range, e.g. $E_{\mathrm{INT}} > 0.1$ eV for a cluster of 49 SIAs (diameter ~ 1 nm) at a distance of about 170 nm, implying a very effective mechanism for the decoration of edge dislocations by glissile SIA loops, as observed in bcc and fcc metals [12,70,71].

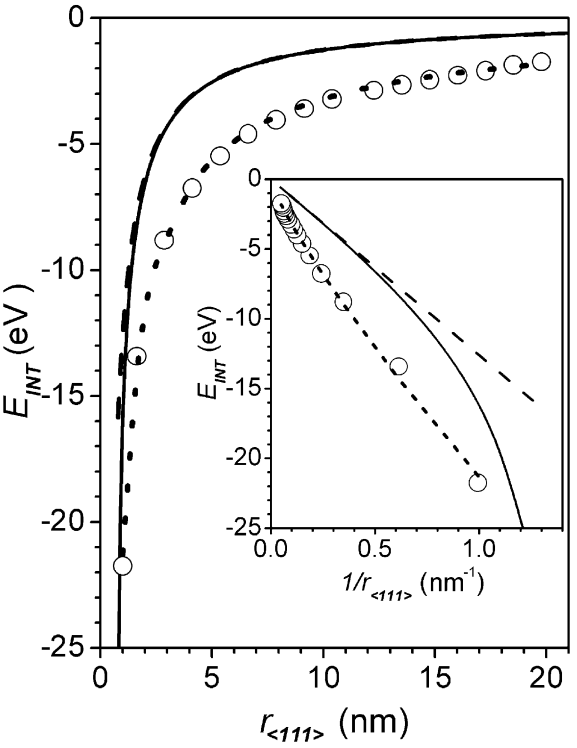

Fig. 4. Interaction energy versus distance between an hexagonal $1/2\langle 1\,1\,0\rangle$ 49-SIA cluster and a $1/2\langle 1\,1\,0\rangle$ dissociated edge dislocation in Cu. Circles indicate modelling results, solid line full integration of dislocation stress field over cluster and dashed line the infinitesimal loop approximation [15].

6. Impact on mechanical properties

The use of atomic-level modelling to investigate the dynamics of dislocations in the presence of defects created by displacement cascades is the most recent application of MD and therefore there are still unresolved issues regarding the validity of the models. Furthermore, not many results have been reported on this topic either.

Interaction between a moving dislocation and small glissile SIA clusters (4–37 SIAs) in Ni was studied in [42] for different dislocation–cluster geometries.

Mechanisms such as cluster drag, cluster absorption on the dislocation line or at previously created jogs, and dislocation pinning and unpinning were demonstrated. The drag of an SIA cluster by a moving edge dislocation, both having the same **b**, was also observed in Fe [35]. The glissile character of clusters in the decoration may allow the decorated dislocation segment to maintain high velocity under the applied stress. Decoration by SIA clusters/loops with the same **b** does not pin the dislocation directly, but by being dragged does increase significantly the interaction cross-section of the dislocation with other microstructure features. Thus, a general picture of interaction of a moving dislocation with damage debris is rather complicated and includes a great variety of reactions between dislocations, clusters other microstructure components (impurities, precipitates, etc.).

A few simulations have been made for the dynamic interaction of a dislocation with vacancy clusters. Thus, interactions between a dissociated edge dislocation and an SFT in Cu have been modelled at zero and non-zero temperatures [32,35,43]. In general, the SFT acts as a rather strong obstacle to dislocation glide, and it may be destroyed and then absorbed by the dislocation, thereby forming a superjog, which reduces the mobility of the dislocation. As an example in Fig. 5 we present the configuration of an SFT in Cu after a $1/2\langle 1\,1\,0\rangle$ edge dislocation has passed through under strain applied at zero temperature [32].

Very recently, the dynamics of glide of an edge dislocation in Fe and the interaction of such a dislocation with a row of voids have been investigated [35]. An example of information obtained from the static simulation of the interaction between a $1/2\langle 1\,1\,1\rangle$ dislocation gliding in a $\{1\,1\,0\}$ plane and spherical voids each of 339 vacancies (diameter ~ 2 nm) and spacing $\sim$40 nm is presented in Fig. 6. The dislocation was moved under

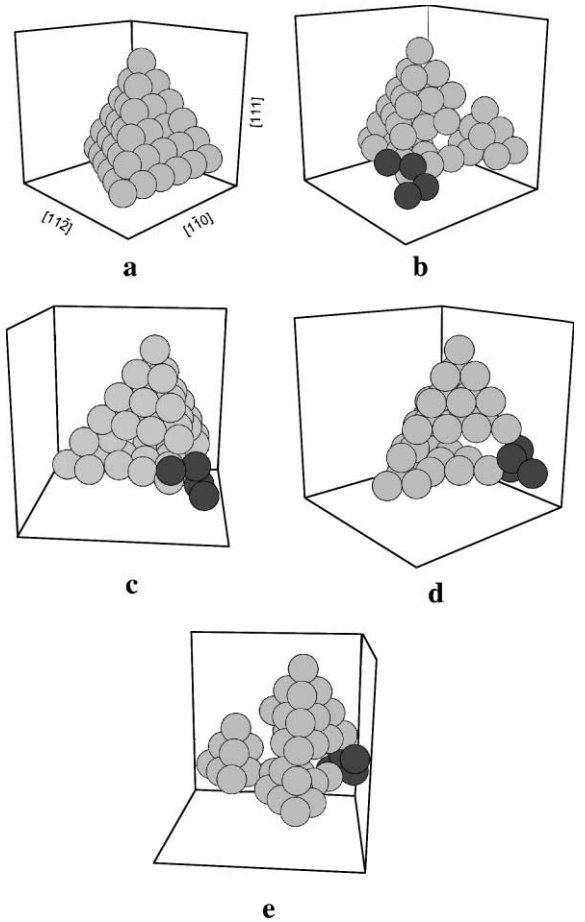

Fig. 5. Configuration of a 21 vacancy SFT before and after (four views, each after 45° rotation around the vertical axis) interaction with a $1/2\langle 1\,1\,0\rangle$ dislocation in Cu. Light spheres indicate position of atoms inside the SFT and dark spheres are atoms in fcc crystal lattice sites [32]: (a) initial; (b) after; (c) after 45°; (d) after 90° and (e) after 135°.

gradually increasing shear strain and the variation of shear stress, crystal energy and plastic displacement is presented. This can be used directly in continuum models of dislocation dynamics. In addition to the static simulations typified by Fig. 6, simulations of a dislocation gliding under stress and meeting a row of obstacles in the form of voids have also been made over wide temperature and stress ranges and the main observations are as follows:

1. At non-zero temperature a straight edge dislocation can move at shear stresses significantly below the Peierls stress, σ_P (for the iron model just discussed $\sigma_P \approx 25$ MPa). An example is presented in Fig. 7. The mechanism of motion can be described as thermal activation of kink nucleation and propagation

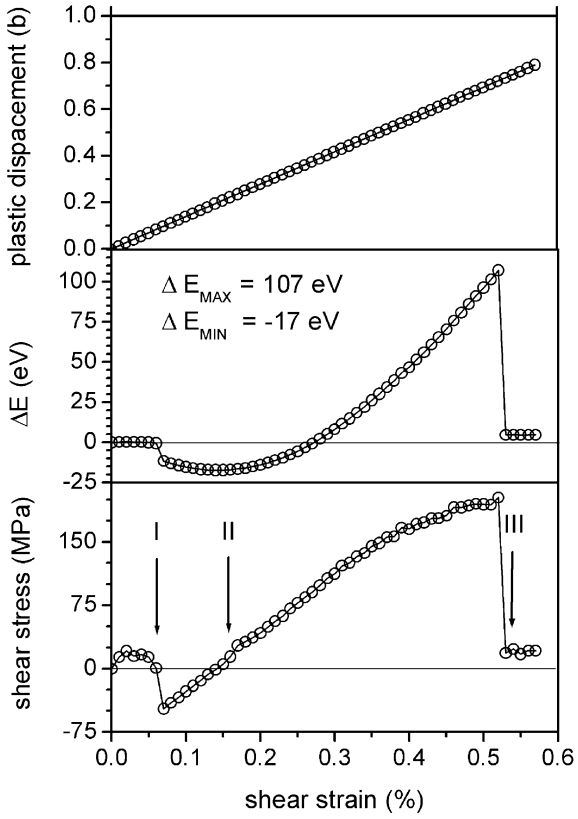

Fig. 6. Shear stress, excess of potential energy in the model crystallite and plastic displacement versus strain during propagation of a $1/2\langle 1\,1\,1\rangle$ edge dislocation through a row of 2 nm void with spacing ~40 nm in Fe [35]. Vertical arrows indicate different stages: I – propagation of the dislocation in perfect crystal, II – the dislocation enters the void and III – the dislocation is released from the void.

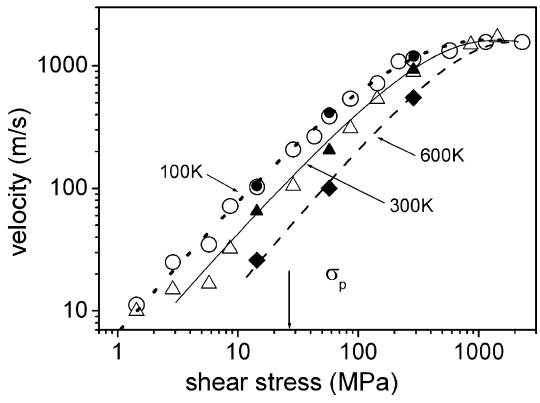

Fig. 7. Velocity of a $1/2\langle 1\,1\,1\rangle$ edge dislocation gliding on a $\{1\,1\,0\}$ plane in Fe versus applied shear stress at different temperatures: circles – 100 K, triangles – 300 K and crosses – 600 K. Open symbols are results for a small crystallite (~300 000 atoms with dislocation line ~9 nm), solid symbols are for a large crystallite (~2 200 000 atoms with dislocation line ~40 nm) [35].

with a low activation energy ~0.01 eV (close to that of the corresponding crowdion): the stress mainly affects the correlation in the motion of the kinks. At low stress ($<0.1\sigma_P$) this motion is similar to the random jumps of kinks, while at high stress ($\geqslant \sigma_P$) the motion of the whole dislocation line becomes uniform.
2. The dislocation-void interaction depends on dislocation velocity, dislocation density, applied stress and temperature.
3. Each time a dislocation crosses a void it climbs due to the absorption of a few vacancies. The height of climb depends on the void size and the void can be completely annihilated after several dislocations passed through it. No significant effects of dislocation velocity or crystal temperature on climb were observed.

Clearly, there are still many questions to be answered with regard to the large variety of interactions that can occur between dislocations and radiation defects. At least one important conclusion can be drawn now: a moving edge dislocation can sweep out both vacancy and interstitial defects. This process may allow understanding of clear channel formation in irradiated metals after a yield drop [72].

7. Conclusions

Atomic-scale computer modelling can be successfully applied to study various stages of main radiation effects in materials: primary damage production, microstructure evolution and changes in deformation behaviour. It can be used to investigate small scale (1–100 nm) fast (<100 ns) processes far beyond the resolution of experimental techniques. The greatest advantage of MD-type computer modelling is that it offers the possibility of identifying and determining the fundamental processes involved in the production, accumulation and interaction of defect clusters with other defect clusters and dislocations. It has been demonstrated unambiguously that defect clusters can be formed directly in displacement cascades. The specific properties of SIA clusters such as high stability, fast thermally activated 1-D glide and long-ranged interactions along their glide prism play an extremely important role in the whole microstructure evolution. The determination of mechanisms of formation of specific microstructures such as rafts of dislocation loops and decoration of edge dislocations by dislocation loops, and mechanisms of interaction between these clusters themselves and with other microstructures such as other radiation defects, impurities, dislocations, etc. provide necessary and unique input for explanation and prediction of radiation effects in materials.

Acknowledgements

Yu.N.O. and D.J.B. acknowledge financial support from the UK Engineering and Physical Sciences Research Council. B.N.S. would like to acknowledge the partial support from the European Fusion Technology Programme.

References

[1] D.J. Bacon, F. Gao, Yu.N. Osetsky, J. Nucl. Mater. 276 (2000) 1.
[2] Yu.N. Osetsky, D.J. Bacon, B.N. Singh, these Proceedings.
[3] Yu.N. Osetsky, M. Victoria, A. Serra, S.I. Golubov, V. Priego, J. Nucl. Mater. 251 (1997) 34.
[4] Yu.N. Osetsky, A. Serra, B.N. Singh, S.I. Golubov, Philos. Mag. A 80 (2000) 2131.
[5] B.D. Wirth, G.R. Odette, D. Maroudas, G.E. Lucas, J. Nucl. Mater. 276 (2000) 33.
[6] Yu.N. Osetsky, A. Serra, V. Priego, MRS Symposium Proc. 527 (1998) 59.
[7] Yu.N. Osetsky, D.J. Bacon, A. Serra, Philos. Mag. Lett. 79 (1999) 273.
[8] Yu.N. Osetsky, D.J. Bacon, A. Serra, B.N. Singh, S.I. Golubov, J. Nucl. Mater. 276 (2000) 65.
[9] N. De Diego, Yu.N. Osetsky, D.J. Bacon, MRS Symposium Proc. 650 (2001) R3.30;
Metall. Mater. Trans. 33A (2002).
[10] C.H. Woo, B.N. Singh, Philos. Mag. A 65 (1992) 889;
B.N. Singh, A.J.E. Foreman, Philos. Mag. A 66 (1992) 975;
H. Trinkaus, B.N. Singh, A.J.E. Foreman, J. Nucl. Mater. 206 (1993) 200;
B.N. Singh, S.I. Golubov, H. Trinkaus, A. Serra, Yu.N. Osetsky, A.V. Barashev, J. Nucl. Mater. 251 (1997) 107;
H. Trinkaus, B.N. Singh, S.I. Golubov, J. Nucl. Mater. 283–287 (2000) 89.
[11] H. Trinkaus, B.N. Singh, A.J.E. Foreman, J. Nucl. Mater. 249 (1997) 91;
H. Trinkaus, B.N. Singh, A.J.E. Foreman, J. Nucl. Mater. 251 (1997) 172;
N.M. Ghoniem, S.H. Tong, J. Huang, B.N. Singh, M. Wen, these Proceedings.
[12] B.N. Singh, J.H. Evans, A. Horsefield, P. Tofft, G.V. Müller, J. Nucl. Mater. 258–263 (1998) 865.
[13] M. Eldrup, B.N. Singh, S.J. Zinkle, T.S. Byun, K. Farrell, these Proceedings.
[14] B.N. Singh, A.J.E. Foreman, H. Trinkaus, J. Nucl. Mater. 249 (1997) 103.
[15] Yu.N. Osetsky, D.J. Bacon, A. Serra, B.N. Singh, MRS Symposium Proc. 653 (2001) Z3.
[16] Yu.N. Osetsky, D.J. Bacon, F. Gao, A. Serra, B.N. Singh, J. Nucl. Mater. 283–287 (2000) 784.
[17] K. Nordlund, L. Wei, Y. Zhong, R.S. Averback, Phys. Rev. B 57 (1998) R13965.
[18] T. Diaz de la Rubia, M.W. Guinan, J. Nucl. Mater. 174 (1990) 151.
[19] F. Gao, D.J. Bacon, P.E.J. Flewitt, T.A. Lewis, J. Nucl. Mater. 249 (1997) 77.

[20] T. Diaz de la Rubia, W.J. Phythian, J. Nucl. Mater. 191–194 (1992) 108;
W.J. Phythian, A.J.E. Foreman, R.E. Stoller, D.J. Bacon, A.F. Calder, J. Nucl. Mater. 223 (1995) 245;
R.E. Stoller, J. Nucl. Mater. 276 (2000) 22;
N. Soneda, S. Ishino, T. Diaz de la Rubia, Philos. Mag. Lett. 81 (2001) 649.
[21] A.J.E. Foreman, C.A. English, W.J. Phythian, Philos. Mag. A 66 (1992) 655.
[22] K. Nordlund, R.S. Averback, J. Nucl. Mater. 276 (2000) 194.
[23] Yu.N. Osetsky, D.J. Bacon, Nucl. Instrum. and Meth. B 180 (2001) 85.
[24] S.J. Wooding, L.M. Howe, F. Gao, A.F. Calder, D.J. Bacon, J. Nucl. Mater. 254 (1998) 191;
S.J. Wooding, D.J. Bacon, W.J. Phythian, Philos. Mag. A 72 (1995) 1261;
S.J. Wooding, D.J. Bacon, Philos. Mag. A 76 (1997) 1033.
[25] N. de Diego, D.J. Bacon, Radiat. Eff. Def. Sol. 141 (1997) 395.
[26] F. Gao, D.J. Bacon, L.M. Howe, C.B. So, J. Nucl. Mater. 294 (2001) 288.
[27] C.S. Becquart, C. Domain, J.C. van Duysen, J.M. Raulot, J. Nucl. Mater. 294 (2001) 274.
[28] F. Gao, D.J. Bacon, Philos. Mag. A 75 (1997) 1603.
[29] M. Spaczer, A. Caro, M. Victoria, T. Diaz de la Rubia, Phys. Rev. B 50 (1994) 13204.
[30] M. Ghaly, K. Nordlund, R.S. Averback, Philos. Mag. A 79 (1999) 795.
[31] Yu.N. Osetsky, A. Serra, V. Priego, J. Nucl. Mater. 276 (2000) 202.
[32] Yu.N. Osetsky, D.J. Bacon, International Workshop on Dislocation–Defect Interactions in Irradiated Metals, Toledo, Spain, April 2000, unpublished.
[33] S. Rao, C. Hernandez, J.P. Simmons, T. Parthasarathy, C. Woodward, Philos. Mag. A 77 (1998) 231.
[34] S.I. Golubov, X. Liu, H. Huang, C.H. Woo, Comp. Phys. Commun. 137 (2001) 312.
[35] Yu.N. Osetsky, D.J. Bacon, 2nd REVE (Reactor for Virtual Experiment) meeting, Segovia, Spain, October 2001, unpublished.
[36] M.S. Daw, S.M. Foiles, M.I. Baskes, Mater. Sci. Rep. 9 (1993) 289.
[37] H. Rafii-Tabar, Phys. Rep. 325 (2000) 239.
[38] M.S. Daw, M.I. Baskes, Phys. Rev. B 29 (1984) 6443.
[39] Yu.N. Osetsky, A.G. Mikhin, A. Serra, Philos. Mag. A 72 (1995) 361.
[40] J.A. Moriarty, Phys. Rev. B 38 (1988) 3199;
J.A. Moriarty, Phys. Rev. B 42 (1990) 361.
[41] M.W. Finnis, J.E. Sinclair, Philos. Mag. A 50 (1984) 45.
[42] D. Rodney, G. Matrin, Phys. Rev. Lett. 82 (1999) 3272;
D. Rodney, G. Matrin, Phys. Rev. B 61 (2000) 8714.
[43] T. Diaz de la Rubia, H. Zbib, T.A. Kraishi, B.D. Wirth, M. Victoria, M.J. Caturla, Nature 406 (2000) 871.
[44] M.J. Norgett, M.T. Robinson, I.M. Torrens, Nucl. Eng. Des. 33 (1975) 50.
[45] M.A. Kirk, I.M. Robertson, M.L. Jenkins, C.A. English, T.J. Black, J.S. Vetrano, J. Nucl. Mater. 149 (1987) 21.
[46] R. Bullough, B.L. Eyre, K. Krishan, Proc. R. Soc. Ser. A 346 (1975) 81.
[47] C.H. Woo, B.N. Singh, H. Heinisch, J. Nucl. Mater. 174 (1990) 190.
[48] M.A. Kirk, M.L. Jenkins, H. Fukushima, J. Nucl. Mater. 276 (2000) 50.
[49] F. Gao, D.J. Bacon, Yu.N. Osetsky, P.E.J. Flewitt, T.A. Lewis, J. Nucl. Mater. 276 (2000) 213.
[50] C.C. Matthai, D.J. Bacon, J. Nucl. Mater. 135 (1985) 173.
[51] V.G. Kapinos, Yu.N. Osetsky, P.A. Platonov, J. Nucl. Mater. 165 (1988) 286.
[52] V.G. Kapinos, Yu.N. Osetsky, P.A. Platonov, J. Nucl. Mater. 170 (1990) 66.
[53] V.G. Kapinos, Yu.N. Osetsky, P.A. Platonov, J. Nucl. Mater. 173 (1990) 229.
[54] V.G. Kapinos, Yu.N. Osetsky, P.A. Platonov, Phys. Stat. Sol. (b) 155 (1989) 373.
[55] V.G. Kapinos, Yu.N. Osetsky, P.A. Platonov, J. Nucl. Mater. 195 (1992) 83.
[56] Yu.N. Osetsky, A. Serra, M. Victoria, V. Priego, S.I. Golubov, Philos. Mag. A 79 (1999) 2259;
Philos. Mag. A 79 (1999) 2285.
[57] V.G. Kapinos, Yu.N. Osetsky, P.A. Platonov, J. Nucl. Mater. 184 (1991) 127;
V.G. Kapinos, Yu.N. Osetsky, P.A. Platonov, Mater. Sci. Forum 97–99 (1992) 97.
[58] N. de Diego, Yu.N. Osetsky, D.J. Bacon, Metall. Trans. 33A (2002) 783.
[59] V.G. Kapinos, Yu.N. Osetsky, P.A. Platonov, J. Nucl. Mater. 184 (1991) 211.
[60] Yu.N. Osetsky, Def. Diffus. Forum 188–190 (2001) 71.
[61] M. Kiritani, J. Nucl. Mater. 216 (1994) 220.
[62] N. de Diego, Yu.N. Osetsky, D.J. Bacon, in press.
[63] N. Soneda, T. Diaz de la Rubia, Philos. Mag. A 81 (2001) 331.
[64] Yu.N. Osetsky, D.J. Bacon, A. Serra, B.N. Singh, S.I. Golubov, Philos. Mag. A., submitted for publication.
[65] A.V. Barashev, Yu.N. Osetsky, D.J. Bacon, Philos. Mag. A 80 (2000) 2709.
[66] S.I. Golubov, B.N. Singh, H. Trinkaus, J. Nucl. Mater. 276 (2000) 78;
A.V. Barashev, S.I. Golubov, H. Trinkaus, Philos. Mag. A 81 (2001) 2515.
[67] Yu.N. Osetsky, D.J. Bacon, MRS Symposium Proc. 650 (2001) R4.2.
[68] M. Pelfort, Yu.N. Osetsky, A. Serra, Philos. Mag. Lett. 81 (2001) 803.
[69] Yu.N. Osetsky, D.J. Bacon, 2000, unpublished.
[70] J.L. Brimhall, B. Mastel, Radiat. Eff. 3 (1970) 325;
B.N. Singh, A. Horsewell, P. Toft, D.J. Edwards, J. Nucl. Mater. 224 (1995) 131.
[71] J.O. Stiegler, E.E. Bloom, Rad. Eff. 8 (1971) 33;
M. Kiritani, J. Nucl. Mater. 216 (1994) 220.
[72] M. Victoria, N. Baluc, C. Bailat, Y. Dai, M.I. Luppo, R. Schäublin, B.N. Singh, J. Nucl. Mater. 276 (2000) 114.